$Zn_{1-x}Mg_xO$ Nanoparticles: Solvothermal Synthesis and Solid Solubility

Xiaoqing Qiu,[1] Yanfeng Xue,[2] Guangshe Li,[1] and Liping Li*[1]
[1]*State Key Structural Chemistry Laboratory, Fujian Institute of Research on the Structure of Matter, Graduate School of Chinese Academy of Sciences, Fujian 350002, P. R. China*
[2]*Department of Physics, Jilin University, Changchun 130023, P. R. China*

(Received December 5, 2006; CL-061430; E-mail: lipingli@fjirsm.ac.cn)

This work reports on the direct preparation of $Zn_{1-x}Mg_xO$ nanoparticles by a solvothermal condition, in which the formation of kinetically stable $Mg(OH)_2$ was significantly suppressed. The reactions do not need any heat treatment procedures. Structural and spectral analyses indicated that Mg^{2+} ions were incorporated into the lattice of ZnO with a solid solubility of about 4.25%. With increasing the Mg content, the E_2 mode of ZnO lattice showed a systematic shift towards higher energies, which was explained in terms of an effective mass model.

Recently, $Zn_{1-x}Mg_xO$ solid solutions have attracted much attention because of their wide band gap and possible band gap modifications for many technological uses such as quantum well structures, superlattices, solar cells, and spintronics.[1,2] Preparation of $Zn_{1-x}Mg_xO$ solid solutions by traditional solid-state reactions meets challenges primarily from the large lattice dismatch between MgO and ZnO. With an aim to extend the solid solutions of Mg^{2+} in ZnO, a variety of techniques including pulsed laser deposition,[3,4] molecular beam epitaxy,[1,5] electrophoresies deposition,[6] and radio frequency magnetron sputtering[7] have been employed to prepare $Zn_{1-x}Mg_xO$. Most of these approaches have shown disadvantages of high expenses and easy formation of accessory metal clusters.[8] Wet chemical methods have been proved to be suitable to produce samples with high uniformity. However, successful direct synthesis of $Zn_{1-x}Mg_xO$ by a wet chemical method is still unavailable,[9] probably because $Mg(OH)_2$ is relatively stable in aqueous solutions. Tomar et al.[10] synthesized the precursors of $Zn_{1-x}Mg_xO$ by solution-based route, but an after-treatment at high temperatures of 650–750 °C is generally needed for formation of $Zn_{1-x}Mg_xO$. It appears very important to find novel effective chemical methods to prepare $Zn_{1-x}Mg_xO$ nanoparticles with advantages such as high uniformity over those produced by physical methods.

Herein, we report on the direct synthesis of $Zn_{1-x}Mg_xO$ nanoparticles with high uniformity and spherical shape via a solvothermal method. Several techniques such as XRD, SEM, TEM, UV–vis, and Raman spectroscopy were used to characterize these samples. We also explored the solid solubility of Mg^{2+} in ZnO lattice and its effect on the band-gap energies and phonon mode frequencies. $Zn_{1-x}Mg_xO$ nanoparticles thus obtained are expected to find potential applications in transparent conductive oxide, optoelectronic and nanoelectronic devices. Details of the experiments and characterizations are given in Supporting Information.[16]

Figure S1[16] shows the Mg contents in $Zn_{1-x}Mg_xO$ nanoparticles determined by ICP as a function of the mole fraction of magnesium acetate in the starting solutions. The Mg contents in $Zn_{1-x}Mg_xO$ nanoparticles increased with the mole fractions of magnesium acetate below 30%. The x values for $Zn_{1-x}Mg_xO$ are 0.00, 0.003, 0.0265, and 0.0425, while the mole fractions of magnesium acetate in the starting solutions are 0, 10, 20, and 30 atom %, respectively. The maximum Mg content in the final products is 4.25% which is consistent with that of about 4% for the thermodynamic solubility limit in phase diagram of ZnO–MgO binary system.[11]

XRD patterns of the samples of various Mg contents are illustrated in Figure S2,[16] in which Miller indices of the diffraction peaks were labeled. It is clear that all patterns matched well the standard data for wurtzite structure. All samples had high crystallinity. The wurtzite structure is not disturbed by the addition of a small amount of Mg^{2+}. The mean sizes of all samples were calculated using the Debye–Scherrer formula from the (101) peak. It is found that the particle sizes are distributed in the range of 20–25 nm regardless of the Mg content. A representative SEM image of $Zn_{1-x}Mg_xO$ samples at $x = 0.0425$ is shown in Figures 1 and S3.[16] It can be clearly seen that all $Zn_{1-x}Mg_xO$ nanoparticles exhibited nearly uniform spherical shapes, which was further confirmed by TEM measurements in Figure 2a. The average grain sizes were all around 20 nm as estimated from SEM observations, which agree with those calculated by XRD analysis. No particles with sizes <7 nm were found. Furthermore, as demonstrated by the corresponding HRTEM in Figure 2b, lattice fringes illustrated the single crystalline nature of these nanoparticles, demonstrating high quality of the as-obtained $Zn_{1-x}Mg_xO$ nanoparticles.

Diffuse reflectance spectra of the samples at room temperature showed significant optical transmission in UV region (Figure 3a). The absorption edges shifted towards higher energies with the increase of Mg content. It is well known that quantum size effect can give rise to a blue shift of the absorption edges. ZnO is a wide band-gap semiconductor. Its quantum size effects generally occur at grain sizes <7 nm.[12] All $Zn_{1-x}Mg_xO$

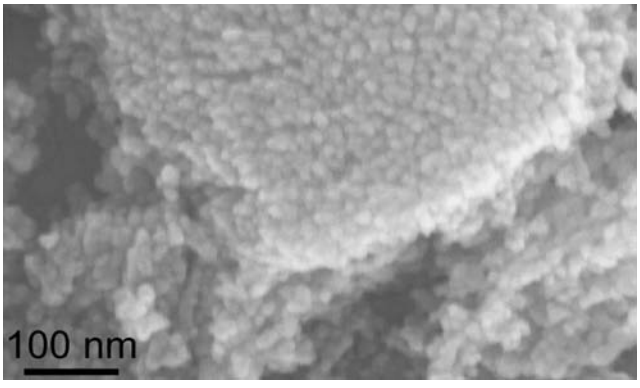

Figure 1. SEM images of the as-prepared $Zn_{1-x}Mg_xO$ nanoparticles at $x = 0.0425$.

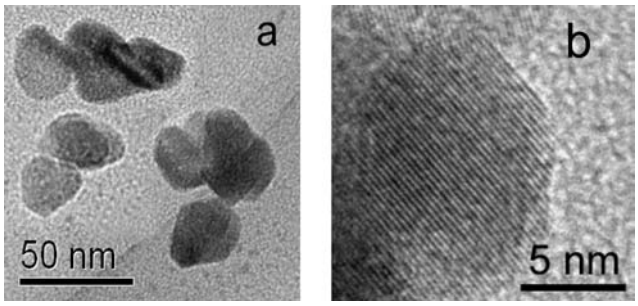

Figure 2. (a) Typical TEM image of $Zn_{1-x}Mg_xO$ nanoparticles at $x = 0.0425$. (b) HRTEM image of an individual particle from (a).

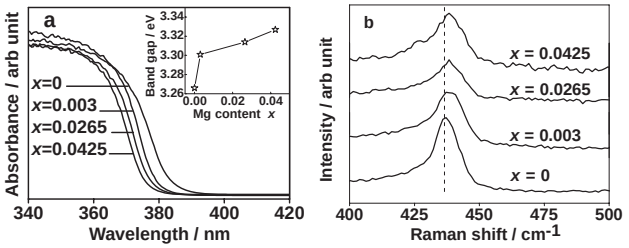

Figure 3. (a) UV–Vis reflectance spectra. (b) Raman spectra of $Zn_{1-x}Mg_xO$ nanocrystals at given Mg content. Inset of Figure 3a shows band-gap energies as a function of Mg content.

nanoparticles reported in this work have similar sizes in the range of 20 to 25 nm, which is well beyond the region for quantum size effects. Therefore, the blue shift of the absorption edges in Figure 3a cannot be ascribed to the quantum size effects. The relationship between the band-gap energies and Mg content is shown in inset of Figure 3a. It is seen that the band gap of $Zn_{1-x}Mg_xO$ was widened abruptly by addition of a little amount of Mg, and its shift is directly pertinent to the Mg^{2+} concentration in wurtzite lattice.

Raman scattering is very sensitive to the microstructures of nanosized materials. Wurtzite structure is of $C_{6\nu}^4$ symmetry and has 4 atoms per unit cell. Consequently, optical phonon modes of $A_1 + E_1 + 2E_2 + 2B_1$ can be expected,[13] in which A_1 and E_1 modes are both Raman and infrared active, while the E_2 modes are Raman active only. For wurtzite structure materials, two Raman peaks are frequently observed at 101 and 437 cm^{-1}. The dominant peak at 437 cm^{-1} is the high-frequency E_2 mode, characteristic of the wurtzite structure. Herein, we investigate the microstructure of $Zn_{1-x}Mg_xO$ nanoparticles using high-frequency E_2 mode as the probe. As indicated in Figure 3b, the E_2 mode for $Zn_{1-x}Mg_xO$ shifted towards higher energies with increasing the Mg content. This observation can be understood by an effective mass model, in which the substitution of Zn^{2+} by Mg^{2+} might reduce the effective mass, thus showing a blue shift in E_2 mode frequency.[10] These results also confirm the incorporation of Mg^{2+} in ZnO lattice.

Concerning the formation mechanism of $Zn_{1-x}Mg_xO$ nanoparticles, it is believed that the formation of the zinc acetate derived precursor[14] is an important step toward the substitution of Mg^{2+} in ZnO lattice. $Zn(Ac)_2 \cdot 2H_2O$ dissolved in hot ethanol may undergo a sequence of reactions, such as solvation by ethanol, formation of the complexes involving the hydroxy and acetate groups, then hydrolysis by traces of water from starting materials, polymerization, and final crystallization into the zinc acetate derived precursors[15] under the solvothermal conditions. Such precursors would be hydrolyzed to crystallize into ZnO by removal of the intercalated Ac^- ions.[14] During the conversion of the precursor, Mg^{2+} ions might be substituted for Zn^{2+} in ZnO lattice to form $Zn_{1-x}Mg_xO$ nanoparticles mainly because of the similarity in ionic radii and charges between Mg^{2+} (0.57 Å) and Zn^{2+} (0.60 Å)[3] and considerable concentration of Mg^{2+} ions in the reaction system.

In summary, we have successfully developed a novel method for direct preparation $Zn_{1-x}Mg_xO$ nanoparticles using a solution-based route. The incorporation of Mg^{2+} in ZnO lattice led to a significant blue shift in band-gap energies. A possible mechanism for the formation of $Zn_{1-x}Mg_xO$ nanoparticles was proposed. This methodology indicates potential applications for other nanoscale binary oxide systems.

This work was financially supported by NSFC under the contract (No. 20671092), a science and technology program from Fujian Province (Nos. 2005HZ01-1 and 2006J0178), and a grant from Hundreds Youth Talents Program of CAS (Li GS).

References and Notes

1 A. Ohtomo, M. Kawasaki, I. Ohkubo, H. Koinuma, T. Yasuda, Y. Segawa, *Appl. Phys. Lett.* **1999**, *75*, 980.
2 T. Gruber, C. Kirchner, R. Kling, F. Reuss, A. Waag, *Appl. Phys. Lett.* **2004**, *84*, 5359.
3 A. Ohtomo, M. Kawasaki, T. Koida, K. Masubuchi, H. Koinuma, Y. Sakurai, Y. Yoshida, T. Yasuda, Y. Segawa, *Appl. Phys. Lett.* **1998**, *72*, 2466.
4 T. Makino, Y. Segawa, M. Kawasaki, A. Ohtomo, R. Shiroki, K. Tamura, T. Yasuda, H. Koinuma, *Appl. Phys. Lett.* **2001**, *78*, 1237.
5 Y. W. Heo, M. Kaufman, K. Pruessner, D. P. Norton, F. Ren, M. F. Chisholm, P. H. Fleming, *Solid-State Electron.* **2003**, *47*, 2269.
6 Y. B. Jin, B. Zhang, S. M. Yang, Y. Z. Wang, J. Chen, H. H. Zhang, C. H. Huang, C. Q. Cao, H. Cao, R. P. H. Chang, *Solid State Commun.* **2001**, *119*, 409.
7 T. Minemoto, T. Negami, S. Nishiwaki, H. Takakura, Y. Hamakawa, *Thin Solid Films* **2000**, *372*, 173.
8 J. H. Kim, H. Kim, D. Kim, Y. E. Ihm, W. K. Choo, *J. Appl. Phys.* **2002**, *92*, 6066.
9 G. Lu, I. Lieberwirth, G. Wegner, *J. Am. Chem. Soc.* **2006**, *128*, 15445.
10 M. S. Tomar, R. Melgarejo, P. S. Dobal, R. S. Katiyar, *J. Mater. Res.* **2001**, *16*, 903.
11 E. R. Segnit, A. E. Holland, *J. Am. Ceram. Soc.* **1965**, *48*, 409.
12 R. Viswanatha, S. Sapra, B. Satpati, P. V. Satyam, B. N. Dev, D. D. Sarma, *J. Mater. Chem.* **2004**, *14*, 661.
13 R. A. Van Leeuwen, C.-J. Hung, D. R. Kammler, J. A. Switzer, *J. Phys. Chem.* **1995**, *99*, 15247.
14 E. Hosono, S. Fujihara, T. Kimura, H. Imai, *J. Colloid Interface Sci.* **2004**, *272*, 391.
15 E. Hosono, S. Fujihara, T. Kimura, H. Imai, *J. Sol-Gel Sci. Technol.* **2004**, *29*, 71.
16 Supporting Information is available electronically on the CSJ-Journal Web site, http://www.csj.jp/journals/chem-lett/index.html.

Published on the web (Advance View) February 3, 2007; doi:10.1246/cl.2007.384